Electronic supplementary information

Dual functional electrochemical sensor based on Au–polydopamine–Fe_3O_4 nanocomposites

Guangfeng Wang,[a,c] Hao Huang,[a] Ge Zhang,[a] Xiaojun Zhang [a] and Lun Wang*[a]

1. Experimental process

1.1. Materials and apparatus. Dopamine, $HAuCl_4 \cdot 4H_2O$, 2–amino–2–hydroxymethylpropane–1,3–diol (Tris) were purchased from Shanghai Chemical Reagent Co., Ltd. Hemoglobin (Hb), IL–6 (Ag), IL–6 antibody (anti–IL–6), α-fetoprotein (AFP), carcinoembryonic antigen (CEA), and human IgG were purchased from Bomei Co., Ltd (Hefei, China). were obtained from Sigma Chemical Co. (St. Louis, MO, USA). A stock solution of 5 mg mL^{-1} Hb was freshly prepared with a 0.025 M phosphate buffer solutions (PBS) (pH 6.5). Bovine serum albumin (BSA, 96–99%), hydrogen peroxide (30%, w/V solution), $K_3Fe(CN)_6$ and $FeCl_3 \cdot 6H_2O$ were purchased from Chemical Reagent Company (Shanghai, China). 0.1 M phosphate buffer solution (PBS, pH 6.86) was used as supporting electrolyte. All other chemicals were of analytical grade and doubly distilled water was used throughout.

Scanning electron microscopy (SEM) images of the electrode surface and electron dispersive spectroscopy (EDS) were obtained using Hitachi S–4800 SEM (operated at 10 kV). Transmission electron micrographs (TEM) were obtained with a Tecnai G220S-TWIN transmission electron microscope (FEI). Fourier transform infrared

(FTIR) spectra were measured on a FTIR–8400S spectrometer in the 480 – 4000 cm^{-1} region using a powered sample on a KBr plate (Japan, Shimadzu). Centrifugation was performed using a HERMLEZ 36 HK apparatus (Wehingen, Germany). Electrochemical measurements were performed on a model CHI660B electrochemical analyser (ChenHua Instruments Co. Ltd., Shanghai, China) controlled by a personal computer with a glassy carbon electrode (GCE) as working electrode, a platinum wire as auxiliary electrode, and a saturated calomel electrode (SCE) as reference electrode. All the electrochemical experiments were carried out at room temperature.

1.2. Preparation of Au–PDA–Fe_3O_4 Nanocomposites. The Fe_3O_4 nanoparticles were prepared by reduction reactions between $FeCl_3$ and ethylene according to the literature [1]. First, 40 mL of 5 mmol $FeCl_3 \cdot 6H_2O$ aqueous solution was mixed with 40 mL ethylene and 3.6 g NaAc. And then the solution was stirred for 30 min. Second, the solution was transferred into a Teflon-lined stainless steel autoclave (50 mL capacity) for hydrothermal treatment at 200□ for 10 h. After the autoclave cool down in room temperature, the formed Fe_3O_4 NPs were washed three times with ethanol, then vacuum-drying. After that, 4 mg of dopamine was dissolved into 2 mL of 10 mg mL^{-1} Fe_3O_4 aqueous solution（10 mM Tris-HCl pH 8.5）and dispersed by sonication for 1 min. The mixture was mechanically stirred at room temperature (20□) for 24 h. And then black precipitate, PDA–Fe_3O_4, was collected by magnet and washed twice with doubly distilled water. In order to induce the Au nanoshell to grow on the surface of PDA–Fe_3O_4, the presynthesized Au NPs used as gold nanoseeds was first dipped onto the PDA–Fe_3O_4 core/shell microspheres. And then $HAuCl_4$ was added for

growing to Au nanoshell. So 20 mL gold seeds solution [2] and 20 mL of 10 mg mL^{-1} PDA–Fe_3O_4 aqueous solution were first mixed and stirred at room temperature (20 ℃) for 2 h and then were collected by magnet and washed by doubly distill water. At last, Au nanoseeds–PDA–Fe_3O_4 (20 mg) was added into 25 mL $HAuCl_4$ aqueous solution (1%wt) and 2mL sodium citrate aqueous solution (1%wt) stirred until the color changed to deep purple to obtain Au–PDA–Fe_3O_4 magnetic nanocomposites. The process of the fabrication is shown in Scheme 1.

1.3. Immobilization of the antibody. The immobilization of the antibody is as follows: 100 μL anti-IL-6 (Ab 320 ng mL^{-1}) was added to the Au–PDA–Fe_3O_4 magnetic nanocomposites (5 mg mL^{-1} in PBS), and stirred on a nonmagnetic mixing device for 12 h at room temperature with slightly stirring, to allow antibodies adhesion to the nanocomposite's surface. The synthesized anti-IL-6-nanocomposite (donated as bionanocomposite) was collected from the solution by placing a magnet under the bottom of the reaction vessel, and the supernatant was discarded. The resulting bionanocomposite was washed with pH=6.86 PBS for 5 times and later the anti-IL-6-Au–PDA–Fe_3O_4 conjugation was re-dispersed in 5 mL pH 6.86 PBS and stored at 4 °C when not in use (Notes: the bionanocomposite was newly prepared for the proposed electrochemical immunosensor each time since it could retain 89.7% of its initial response at 4 °C after a storage period of 14 days.) The fabricated procedure of bionanocomposite is shown in Scheme 1.

1.4. Fabrication of Immunosensors. (1) The bare glassy carbon electrode (GCE) was polished with 0.05 μm alumina powders, and then rinsed ultrasonically with

water, absolute ethanol and twice distilled water, respectively. (2) PDA was coated on GCE according to the literature with a little modification [3]. Briefly, 0.5 mg mL^{-1} dopamine was dissolved in 10 mmol L^{-1} pH 8.5 Tris–HCl, and GCE was immersed into the solution for 24 h. The coated surfaces were rinsed with water, dried by N_2 gas and then PDA/GCE was obtained and PDA was used as the substrate to absorb the bionanocomposite. (3) The following experiments were undertaken to develop the immunoassay that facilitates the detection of an unknown amount of sample IL-6 with a fixed amount of anti-IL-6-tagged magnetic biocomposite. 20 μL of 0.1 mg mL^{-1} bionanocomposite solution (50 mmol L^{-1} pH 6.86 PBS) was spread onto the PDA/GCE surface. The electrode was incubated at 4 °C in a moisture atmosphere. After incubation for at least 12 h, they were rinsed with pH 6.8 PBS, 0.05% Tween (PBST) to remove physically absorption. (4) In this work, we used Hb instead of BSA as the blocking reagent. So the electrodes were then blocked with 5 mg mL^{-1} Hb solution for 1 h at room temperature, and washed with PBST. All washing steps were optimized to minimize nonspecific binding (NSB) to achieve the necessary sensitivity. After aspiration, bionanocomposite modified electrodes incubated with 10 μL of the detecting Ag samples for 1 h at 37 °C, by the binding reaction between Ab_1 and Ag. The immunocomplexes were then formed and observed after incubating the sensing surface with various concentration of IL-6. (5) The electrodes were washed thoroughly with PBST to remove nonspecifically bound conjugations, which could cause a background response before measurement. The procedure of the immobilization of Ab_1 was as the Scheme 1 shows.

1.5. Electrochemical Detection of the antigen. The detection of IL-6 is shown in Scheme 1. Electrochemical detection was according to the literature [4] with a little modification involved first oxidation of the AuNPs at 1.2 V for 120 s in 0.1 M NaCl (10 μL) and subsequent reduction to Au^0 at 0.35 V (vs. the SCE) using differential pulse voltammetry (DPV), scanning from 0.8 to 0.0 V with an amplitude of 50 mV and a step potential of 4.0 mV at 15 Hz.

2. **Characterization of the nanocomposites**

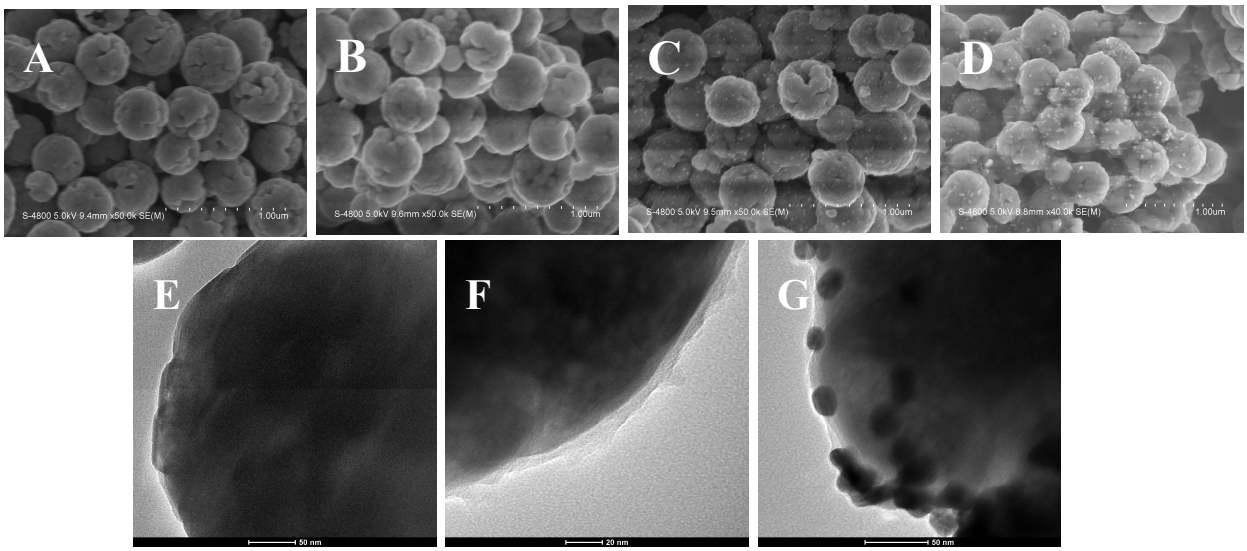

Figure S1 SEM images of Fe_3O_4 NPs (A), PDA–Fe_3O_4 (B), Au–PDA–Fe_3O_4 (C), Ab_1–Au–PDA–Fe_3O_4 (D) and TEM images of Fe_3O_4 NPs (E), PDA–Fe_3O_4 (F), Au–PDA–Fe_3O_4 (G).

Figure S1 showed the typical SEM and TEM images of Fe_3O_4 NPs, PDA–Fe_3O_4 NPs, and Au–PDA–Fe_3O_4 nanocomposites. The SEM images in Figures S1 A and B showed that the Fe_3O_4 NPs and PDA–Fe_3O_4 NPs were spherical with uniform size and shape. The obtained Fe_3O_4 NPs showed that the average diameter was about 200

nm. As shown in Figure S1B, PDA–Fe_3O_4 NPs with well-defined core/shell structures were successfully synthesized. By comparing Figure S1E and F, we found that there exists a clear interface between the PDA shell and the Fe_3O_4 core as shown in Figure S1F and the average thickness of the PDA shell was about 12 nm, indicating that Fe_3O_4 core was well encapsulated by the coating layer. The small particles (e.g. 13 nm in size) coated on the PDA-Fe_3O_4 NPs were Au NPs as shown in Figure S1C and Figure S1G. And after the antibody was modified onto the Au–PDA–Fe_3O_4 nanocomposites, the surface of the bionanocomposites became rougher (Fig. S1D). The hypothesis was further confirmed by the spectrums of electron dispersive spectroscopy (EDS) of different composites in Figure S2. Fig. S2 A, B and C is the EDS of Fe_3O_4, PDA–Fe_3O_4 and Au–PDA–Fe_3O_4, respectively. As shown in Fig. S2 C, the peaks of Au, Fe, and O elements present, suggests that the hybrid spheres may contain Fe_3O_4 and Au. While the N signals prove the presence of PDA existed.

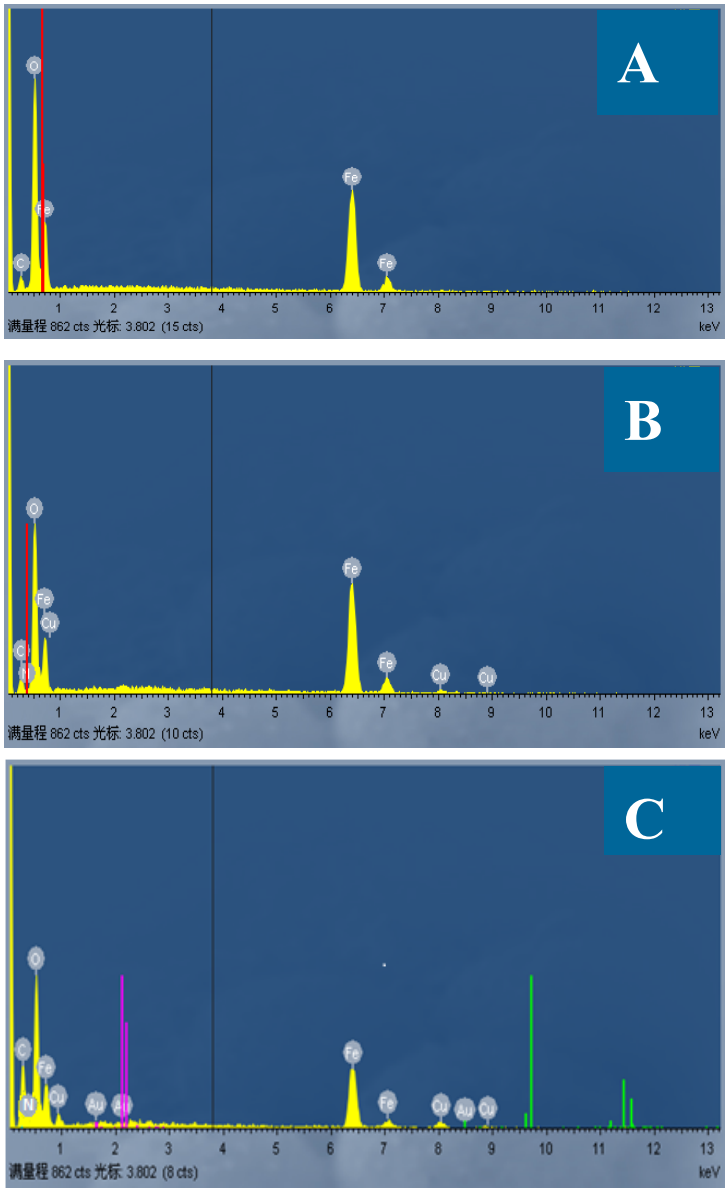

Fig. S2 EDS of Fe_3O_4 (A), PDA–Fe_3O_4 (B) and Au–PDA–Fe_3O_4 (C)

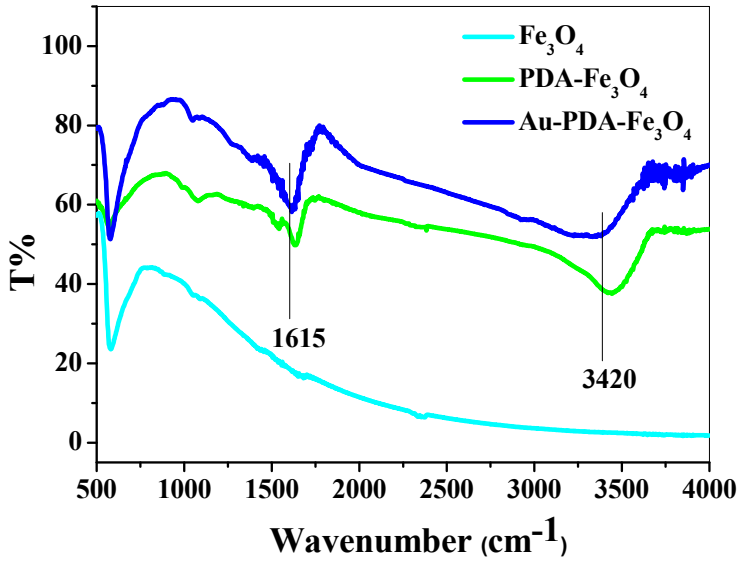

Fig. S3 FT-IR spectra of the prepared pure Fe_3O_4, PDA–Fe_3O_4, and Au–PDA–Fe_3O_4

Figure S3 gives the FT-IR spectra of the prepared pure Fe_3O_4, PDA–Fe_3O_4, and Au–PDA–Fe_3O_4 composites. As shown in Figure S3, the FTIR spectrum of pure Fe_3O_4 shows the stretching frequencies for Fe–O bond at 572 cm^{-1}, which tally with the published results [6]. While PDA presents intense absorption features: around 1615 cm^{-1} from aromatic rings and around 3420 cm^{-1} from catechol –OH groups, which is accordance with the literature [7]. When PDA–Fe_3O_4 was combined with Au NPs, the peaks of PDA shifted to low wavenumber, which are directly related to the differences in electron density. As the electron density donator, Au NPs make the electron cloud of PDA more delocalized. A similar change in the FT-IR absorption spectra of PDA was observed after combining with Au NPs. Overall, these FT-IR

spectra provided supportive evidence that PDA–Fe_3O_4 and Au–PDA–Fe_3O_4 nanocomposites have been successfully prepared.

3. EIS characterization

Impedance spectroscopy was reported as an effective method to monitor the feature of surface allowing the understanding of chemical transformation and processes associated with the conductive electrode surface. Fig. S4 compares the EIS obtained for $K_3Fe(CN)_6$ at different electrodes.

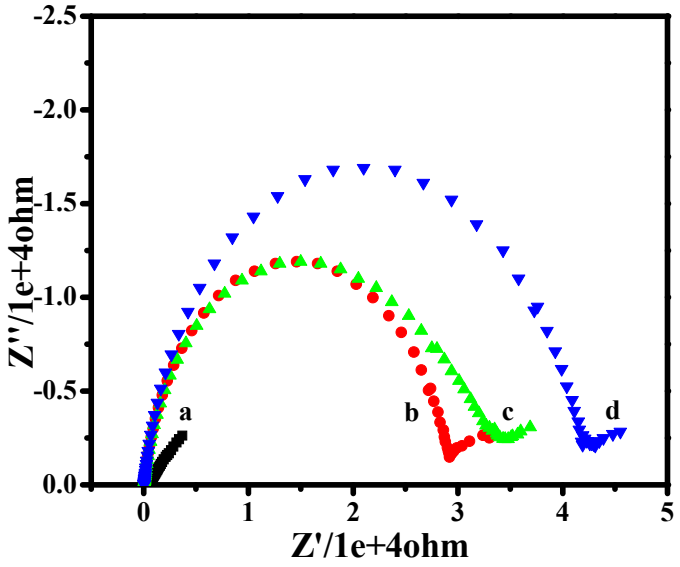

Fig. S4 The EIS results of the bare GCE (curve a), PDA/GCE (curve b), Ab_1–Au–PDA–Fe_3O_4/PDA/GCE (curve c), and Hb/Ab_1–Au–PDA–Fe_3O_4/PDA/GCE (curve d), in 5.0 mmol L^{-1} $Fe(CN)_6^{3-/4-}$ containing 0.10 M KCl solution, respectively.

4. Comparison of the determination results to H_2O_2 of other Hb modified electrode

Films	Detection ranges ($\mu molL^{-1}$)	Detection limits ($\mu molL^{-1}$)	References
Hb–Titanate Composite	20–3200	8	8
Hb/Au NPs/Multiwall Carbon Nanotubes/Chitosan	0.5–2000	0.21	9
Hb/gold colloid/L–cysteine/gold colloid/NPs Pt–chitosan	0.14–6600	0.045	10

Hb–triacetone triperoxide	19.58–117.45	5.53	11
Hb–mesoporous carbon	1.2–57	0.6	12
Hb–$CaCO_3$ multilayer	10–120	5.0	13
Hb niobate	25–3000	1.7	55
Silver NPs–chitosan film	0.75–216	0.5	14
Au–PDA–Fe_3O_4	0.01–10	0.007	our work

Table S1 Comparison of the determination results to H_2O_2 of other Hb modified electrode

4. The application of the electrochemical immunosensor in real samples

Table S2 The recovery of the prepared immunosensor in human serum.

Sample[a]	Standard value of IL-6 (ng mL^{-1})	Found[b] (ng mL^{-1})	Recovery (%)
1	0.5	0.59	118.0
2	5.0	5.5	110.0
3	10.0	10.9	109.0
4	20.0	19.1	95.5
5	60.0	59.2	98.7
6	80.0	82.5	103.1

[a] Samples were appropriately diluted with 0.025 M PBS (pH 6.86).

[b] The values shown here are the average values from 5 measurements.

Table S3 Experimental results of different methods obtained in serum samples

Serum sample [a]	1	2	3	4	5
Immunosensor($ng.mL^{-1}$) [b]	5.5	10.9	19.1	59.2	82.5
ELISA ($ng.mL^{-1}$) [b]	5.28	11.2	20.2	57.8	84.7
Relative deviation (%)	+4.16	−2.60	−5.44	+2.42	−2.60

[a] Samples were appropriately diluted with 0.025 M PBS (pH 6.86).

[b] The values shown here are the average values from 5 measurements

Reference

1. S. Liu, R. Xing, F. Lu, R. K. Rana, J. J. Zhu. *J. Phys. Chem. C* 2009, **113**, 21042-21047.

2. G. Frens, *Nature Phys. Sci.* 1973, **241**, 20-22.

3. H. Lee, S. M. Dellatore, W. M. Miller, P. B. Messersmith, *Science* 2007, **318**, 426-430.

4. A. J. Ho, H. C. Chang, N. Y. Shih, L. C. Wu, Y. F. Chang, C. C. Chen, C. Chou. *Anal. Chem.* 2010, **82**, 5944–5950.

5. D. P. Tang, R. Yuan, Y. Q. Chai. *J. Phys. Chem. B* 2006, **110**, 11640-11646.

6. B. Fei, B. T. Qian, Z. Y. Yang, R. H. Wang, W. C. Liu, C. L. Mak, J. H. Xin. *Carbon* 2008, **46**, 1795-1797.

7. Y. Wu, Q. Gao, L. Shi, L. Gao. *Electroanalysis* 2009, **21**, 904–908.

8. S. Chen, R. Yuan, Y. Chai, B. Yin, Y. Xu. *Electroanalysis* 2008, **20**, 2141–2147.

9. G. Yang, R. Yuan, Y. Q. Chai. *Colloids and Surf., B* 2008, **61**, 93–100.

10. F. Jian, Y. Qiao, R. Zhang. *Sens. and Actuators, B* 2007, **124,** 413–420

11. J. J. Feng, J. J. Xu, H. Y. Chen. *Biosens. and Bioelectron.* 2007, **22**, 1618–1624.

12. Y. Ding, W. Jia, H. Zhang, B. Li, Z. Gu, Y. Lei. *Electroanalysis* 2010, **22**, 1911–1917.

13. L. Gao, Q. Gao. *Biosens. Bioelectron.* 2007, **22**, 1454–1460.

14. C. Yu, X. Zhou, H. Gu. *Electrochim. Acta* 2010, **55**, 8738–8743.